



Anna Szafarczyk

## THE ACCURACY OF STRAIN TENSOR DETERMINED IN THE LANDSLIDE AREAS

AGH University of Science and Technology  
szafarcz@agh.edu.pl

**Keywords:** landslide, strain tensor, geodetic measurements

### Abstract

Geodetic surveys, performed serially in the area subject to deformations, allow to determine deformation rates, of which, for most building structures, horizontal strains appear to be the most important ones. There are horizontal tensile and compressive strains. Tensile strains of land cause the greatest damage to residential buildings, resulting in hairline and larger cracks, or even construction disasters in extreme cases. Depending on the adopted surveying method, it is possible to determine the values of strains more or less accurately. For the strains with small values it is necessary to determine the length directly (from the total station measurement), whereas for the strains with large values it is possible to use the GPS measurement results. The article presents the surveying method and the measurement results of landslide fragments deformation. Geodetic points were stabilized in the form of a control network called a rosette. Measurements of the rosette were performed and, on their basis, horizontal strains were calculated for the directions of the stabilized sides. The further stage included determining surface strain tensor components, from which it is possible to determine the direction and the values of the occurring extreme strain.

## DOKŁADNOŚĆ OKREŚLANIA SKŁADOWYCH TENSORA ODKSZTAŁCENIA WYZNACZANEGO NA TERENACH OSUWISKOWYCH

**Słowa kluczowe:** osuwisko, tensor odkształcenia, pomiary geodezyjne

### Abstrakt

Pomiary geodezyjne, wykonywane seryjnie na terenie podlegającym deformacjom, pozwalają na wyznaczenie wskaźników deformacji, z których najbardziej istotnym dla większości obiektów budowlanych jest odkształcenie poziome. Wyróżniamy odkształcenia poziome rozciągające oraz ściskające. Odkształcenia rozciągające terenu powodują największe uszkodzenia w obiektach budownictwa mieszkaniowego, prowadząc do powstania rys, pęknięć a w skrajnym przypadku nawet katastrofy budowlanej. W zależności od przyjętej geodezyjnej technologii pomiaru możliwe jest wyznaczenie wartości odkształceń z mniejszą lub większą dokładnością. Dla odkształceń o małych wartościach konieczne jest wyznaczenie długości w sposób bezpośredni (z pomiaru tachimetrycznego), natomiast dla odkształceń o wartościach dużych możliwe jest wykorzystanie wyników pomiarów GPS. W artykule przedstawiono metodę i wyniki pomiaru deformacji fragmentów osuwiska. Zastabilizowano punkty geodezyjne w formie sieci pomiarowej zwanej prostokątną rozetą geodezyjną. Wykonano pomiary rozety i obliczono na ich podstawie odkształcenia poziome na kierunkach zastabilizowanych boków. W dalszym etapie wyznaczono składowe powierzchniowego tensora odkształceń, z których możliwe jest wyznaczenie kierunku i wartości występującego odkształcenia ekstremalnego.



## 1. INTRODUCTION

Surface mass movements, commonly referred to as landslides, are a phenomenon of variable dynamics (Teza et al., 2008; Dong et al., 2009; Yenes et al., 2009; Stumpf et al., 2013; Kostić et al., 2014; Prokešova et al., 2010; Szafarczyk et al., 2013). They become activated as a result of the occurrence of natural factors, but can also be caused by human activity. A particularly important aspect of the study of landslides is their impact on objects resulting from human activity as well as on engineering and geological conditions. For this purpose, geodetic measurements with the use of various technologies and instruments are carried out in the landslide areas (Wasowski and Bovenga, 2015; Ramesh, 2014; Gili et al., 2000; Zhu et al. 2011; Ćmielewski, 2013). The results of the performed measurements are used not only to describe the phenomenon itself, but also to give grounds for risk assessment for the buildings located in areas subject to deformation.

## 2. DESCRIPTION OF THE PHENOMENON

Most often, to describe the kinematics of surface mass movements, the values of the horizontal component of the displacement vector  $u$  and the values of the displacement rate  $v_u$  are used (Wang and Lin, 2011; Okamoto et al., 2004; McColl, 2015). These data are sufficient to inform about the landslide activity or lack thereof.

Considering the problem of landslides from the point of view of the danger posed to building structures and infrastructure, displacement values are no longer as important as other surface deformation rates.

For slender structures (e.g. powerline poles), the most important rate is the tilt, and specifically its change causing a gradual tilting of the structure until it falls over. For linear objects with the given initial slope (e.g. sewage system), the most important are the slopes associated with uneven terrain subsidence.

For most residential buildings, however, the most significant deformation rate is linear strain, especially linear tensile strain, resulting in damage in the form of cracks and scratches. Therefore, the results of geodetic measurements, depending on the purpose they are to serve, must be based on various methods and calculation

techniques, with the result being reliable and allowing for the correct interpretation of the ongoing changes as well as of their impact on the environment.

## 3. DETERMINING STRAIN TENSOR BASED ON THE RESULTS OF GEODETIC MEASUREMENTS

Determination of the value of linear strain  $\varepsilon$ , based on the results of geodetic measurements, involves measuring the length of a given segment in two different moments of time, and then determining the relative change in this length, according to the following relationship (Gustkiewicz, 1980):

$$\varepsilon = \frac{l - l_0}{l_0}, \quad (1)$$

where:

$l_0$  – segment length in the initial measurement,  
 $l$  – segment length after the deformation.

The length of the segment  $l$  can be measured directly (with a total station), or calculated from coordinates (e.g. determined based on GPS measurements) according to the formula (Kajetanowicz et al., 2008):

$$l = \sqrt{(x_B - x_A)^2 + (y_B - y_A)^2}. \quad (2)$$

Depending on the manner of determining the length, the error varies.

In the case of a direct measurement (with a total station) the mean error in the measured length is (Wanic, 2007):

$$m_l = \pm a + b \cdot 10^{-6} l, \quad (3)$$

where:

$a$  – a fixed component (instrumental errors and error of determining instrument adjustments of the range-finder),

$b$  – a coefficient proportional to the measured length, and in the case of calculating the length from the Cartesian coordinates, the error is determined by differentiating the equation (2) with respect to the individual coordinates of the points:

$$\frac{\partial l}{\partial y_B} = \frac{y_B - y_A}{\sqrt{(y_B - y_A)^2 + (x_B - x_A)^2}},$$

$$\frac{\partial l}{\partial y_A} = -\frac{y_B - y_A}{\sqrt{(y_B - y_A)^2 + (x_B - x_A)^2}},$$

$$\frac{\partial l}{\partial x_B} = \frac{x_B - x_A}{\sqrt{(y_B - y_A)^2 + (x_B - x_A)^2}},$$

$$\frac{\partial l}{\partial x_A} = -\frac{x_B - x_A}{\sqrt{(y_B - y_A)^2 + (x_B - x_A)^2}}.$$

Using the law of error propagation for independent observations:

$$m_l^2 = \left(\frac{\partial l}{\partial y_B}\right)^2 m_{y_B}^2 + \left(\frac{\partial l}{\partial y_A}\right)^2 m_{y_A}^2 + \left(\frac{\partial l}{\partial x_B}\right)^2 m_{x_B}^2 + \left(\frac{\partial l}{\partial x_A}\right)^2 m_{x_A}^2,$$

a relationship is obtained:

$$m_l^2 = \pm \left(\frac{y_B - y_A}{l}\right)^2 (m_{y_B}^2 + m_{y_A}^2) + \left(\frac{x_B - x_A}{l}\right)^2 (m_{x_B}^2 + m_{x_A}^2), \quad (4)$$

and assuming the same values of coordinate errors

$$m_{y_B} = m_{y_A} = m_{x_B} = m_{x_A}$$

and marking them as  $m$  we obtain

$$m_l^2 = 2m^2,$$

and hence the error in the measured length is

$$m_l = \pm\sqrt{2}m. \quad (5)$$

The value of the error in the measured length determined in such a manner affects the accuracy of the strain value calculated at a later stage.

After equation (1) has been differentiated, it is obtained:

$$\frac{\partial \varepsilon}{\partial l} = \frac{1}{l_0},$$

$$\frac{\partial \varepsilon}{\partial l_0} = -\frac{1}{l_0} - \frac{l - l_0}{l_0^2}.$$

Using the law of error propagation, assuming that the length before deformation  $l_0$ , and after the deformation  $l$  is affected by the same error  $m_l = m_{l_0}$ , the relationship for calculating a linear strain error is obtained:

$$m_\varepsilon = \pm m_l \frac{\sqrt{2 + 2\varepsilon + \varepsilon^2}}{l_0}. \quad (6)$$

Based on the relationship derived above, it can be concluded that the value of the strain error is determined by: the value of the error in the length of the measuring segment, and the value of the strain and the measured length.

Assuming the occurrence of a case in which we observe a strain of the same value, it can be concluded that a strain determined based on direct measurements of length is determined with a greater precision (smaller mean error) than the strain calculated based on the length calculated from the coordinates of points, which are the ends of a given measurement segment.

The calculated values of linear strain apply only to specific sides, for which they were determined. The knowledge of a strain in any direction, originating at a specific point (i.e. the knowledge of the strain tensor components) is possible if the values of at least three linear strains, together with the azimuths of their occurrence, will be determined. This is accomplished by performing a measurement on the sides of the so-called strain gauge rosettes of various shapes (Fig. 1).

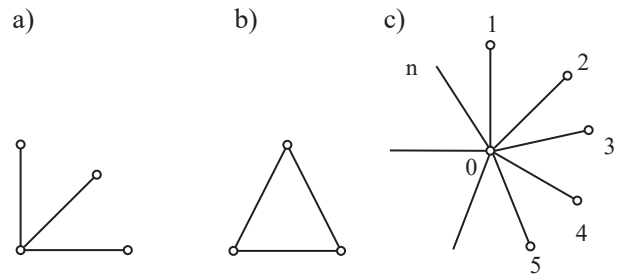


**Fig. 1.** Types of strain gauge rosettes: a) rectangular rosette, b) delta rosette, c) rosette with the central point.

**Rys. 1.** Rodzaje geodezyjnych rozet pomiarowych: a) rozeta prostokątna, b) rozeta trójkątna, c) rozeta z punktem centralnym.

These structures are successfully used in various types of surveys (Hejmanowski, 2005; Kontny et al., 2014; Kwinta, 2012; Szafarczyk, 2013; Pielok and Szafarczyk, 2004).

For each side of a known value of the linear strain, an equation is formulated in the following form (Gustkiewicz J. 1980):

$$\varepsilon_i = \varepsilon_{11} \cos^2 \phi_i + 2\varepsilon_{12} \cos \phi_i \sin \phi_i + \varepsilon_{22} \sin^2 \phi_i, \quad (7)$$

where:

$\varepsilon_i$  – linear strain on the side  $i$ ,

$\varepsilon_{11}, \varepsilon_{12}, \varepsilon_{22}$  – strain tensor components,

which in the matrix form takes the following form:

$$\begin{pmatrix} \varepsilon_{11} & \varepsilon_{12} \\ \varepsilon_{21} & \varepsilon_{22} \end{pmatrix}. \quad (8)$$

The values of the components on the main diagonal:

$$\varepsilon_{11} = \frac{\partial u_x}{\partial x} \quad \text{and} \quad \varepsilon_{22} = \frac{\partial u_y}{\partial y}$$

are interpreted as strains on the directions of the axis of the adopted coordinate system, while the component outside the diagonal of the matrix (symmetric)  $\varepsilon_{12} = \varepsilon_{21} = \frac{1}{2} \left( \frac{\partial u_y}{\partial x} + \frac{\partial u_x}{\partial y} \right)$  is interpreted as half of the change in the straight angle between the axes of the system.

Based on the known coordinates of the strain tensor it is possible to determine the values of the extreme strain  $\varepsilon_{\max}$  and  $\varepsilon_{\min}$  originating from a given point by the formula:

$$\left. \begin{matrix} \varepsilon_{\max} \\ \varepsilon_{\min} \end{matrix} \right\} = \frac{\varepsilon_{11} + \varepsilon_{22}}{2} \pm \frac{1}{2} \left[ (\varepsilon_{11} - \varepsilon_{22})^2 + 4\varepsilon_{12}^2 \right]^{\frac{1}{2}} \quad (9)$$

together with the angle  $\beta$  between the direction of the occurrence of the maximum strain  $\varepsilon_{\max}$  and the  $x$  axis of the coordinate system:

$$\beta = \frac{1}{2} \operatorname{arctg} \frac{2\varepsilon_{12}}{\varepsilon_{11} - \varepsilon_{22}} \quad (10)$$

as well as the value of the shear  $\gamma_{ekstr}$ :

$$\gamma_{ekstr} = \varepsilon_{\max} - \varepsilon_{\min} = \pm \left[ (\varepsilon_{11} - \varepsilon_{22})^2 + 4\varepsilon_{12}^2 \right]^{\frac{1}{2}}. \quad (11)$$

Strain gauge rosettes were used to determine the deformation of the landslide area. This was implemented through examination of two landslides differing in the degree of their activity and the cause of their emergence. The objective of the performed analyses was to assess the significance of these deformations depending on the measurement technology and its accuracy.

#### 4. LANDSLIDE ON THE NATURAL SLOPE IN MILÓWKA

Landslide of Prusów natural mountainside in Milówka (Poland, Silesia, Żywiec district) became active in May 2010 after a period of heavy rains. Morphometric parameters of the landslide have been shown in Table 1.

**Table 1.** Morphometric parameters of the landslide in Milówka

**Tabela 1.** Parametry morfometryczne osuwiska w Milówce

Parameter	
Area [ha]	12
Length [m]	470
Width [m]	276
Maximum height [m above sea level]	715
Minimum height [m above sea level]	598
Inclination [°]	25
Azimuth [°]	170

In September 2010, in the landslide area and in its immediate vicinity 74 points were established, whose X, Y, H location was being determined on a half-yearly basis for a period of three years to obtain maximum total displacement values equal to 4 cm. In the central part of the landslide, a rectangular rosette was established with the points marked with the following numbers: 100, 200, 300 and 400 (Fig. 1).

The rosette measured all the horizontal angles and all the lengths. Strict adjustment of the observations was performed in three versions: linear, angular and angular-linear. Of the three adjustment results, this one was chosen in which the adjusted lengths were affected by the smallest errors (Tab. 2).

Basing on the adjusted lengths, linear strain values were calculated on the sides of the rosette, together with errors (Tab. 3), as well as the strain tensor components, the values of extreme deformation, shear value  $\gamma$  and the angle  $\beta$  (Tab. 4).

On the basis of the calculated tensor components, strain distribution has been plotted (Fig. 2)

The rectangular rosette established over the central part of the landslide in Milówka revealed both compressive and tensile strains. The maximum value of the

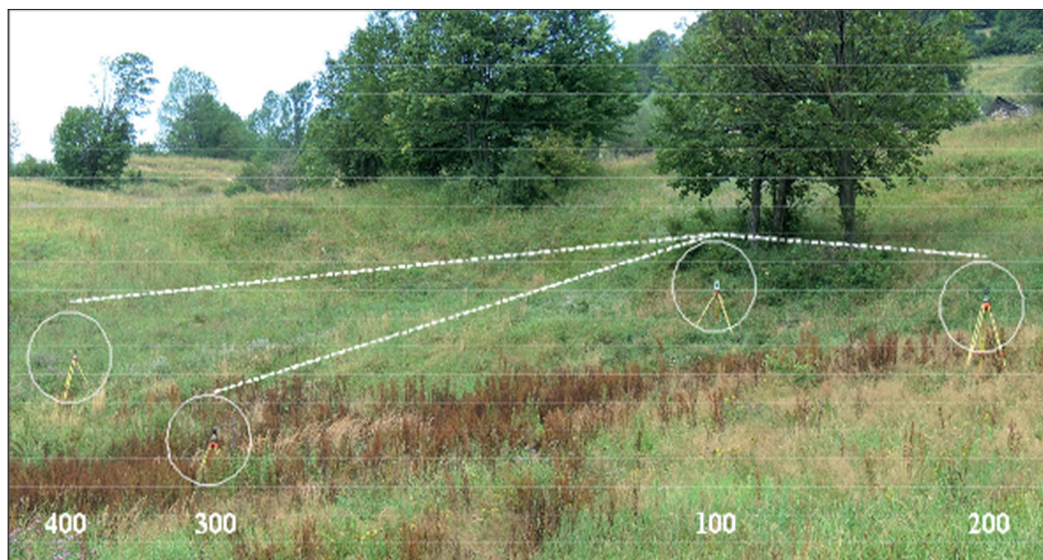


**Fig. 1.** Location of the rectangular rosette in Milówka, together with marking of the points it is created by (Pałka and Skulich 2013)  
**Rys. 1.** Usytuowanie rozety prostokątnej na tle granic osuwiska w Milówce wraz z oznaczeniem punktów ją tworzących (Pałka, Skulich 2013)

**Table 2.** Summary of the adjusted lengths of the sides of the rosette, together with errors in each measurement series  
**Tabela 2.** Zestawienie wyrównanych długości boków rozety wraz z błędami w poszczególnych seriach pomiarowych

Side	Measurement series (date of performance)		
	I (29 IX 2011)	II (1 VIII 2012)	III (10 X 2014)
100–200	20,023m±0,3 mm	20,026m±2,0 mm	20,028m ±1,4 mm
100–300	19,839m±0,3 mm	19,843m±2,0 mm	19,847m ±1,3 mm
100–400	20,034m±0,3 mm	20,034m±2,0 mm	20,040m ±1,5 mm

**Table 3.** Linear strains on the sides of the rosette, with errors  
**Tabela 3.** Odształcenia liniowe na bokach rozety wraz z błędami

Side	Linear strain in the period I–II [mm/m] ± error [mm/m]	Linear strain in the period I–III [mm/m] ± error [mm/m]
100–200	0,17 ±0,15	0,24 ±0,11
100–300	0,22 ±0,16	0,43 ±0,11
100–400	0,00 ±0,14	0,32 ±0,12

tensile strain (observed in the period I–III) was 0.43 mm/m on the direction of the azimuth equal to 24 gon. This corresponds to the direction of the slope. However, given the accuracy of the determined strain, most of them (except 0.43 mm/m) must be recognized as insignificant

from a statistical point of view. The determined strains fall within the limits of the error. Therefore, for the above case it can be concluded that, in the specified time period, in the vicinity of the established strain gauge rosette, the landslide was not active.

**Table 4.** Strain tensor components and the values of  $\gamma$  and  $\beta$  determined for the state on August 1, 2012, and October 10, 2014 relative to the first measurement series performed on 29 September, 2011 for the rectangular rosette in Milówka

**Tabela 4.** Składowe tensora odkształcenia oraz wartości  $\gamma$  i  $\beta$  wyznaczone dla stanu w dniu 1 VIII 2012 oraz 10 X 2014 względem pierwszej serii pomiarowej wykonanej dnia 29 IX 2011 dla rozety prostokątnej w Milówce

State as of (date)	$\varepsilon_{11}$ [mm/m]	$\varepsilon_{12} = \varepsilon_{21}$ [mm/m]	$\varepsilon_{22}$ [mm/m]	$\varepsilon_{\max}$ [mm/m]	$\varepsilon_{\min}$ [mm/m]	Gamma [-]	Beta [g]
2012-08-01	0,24	-0,02	-0,07	0,24	-0,07	0,32	196,32
2014-10-10	0,39	0,10	0,17	0,43	0,13	0,30	24,09

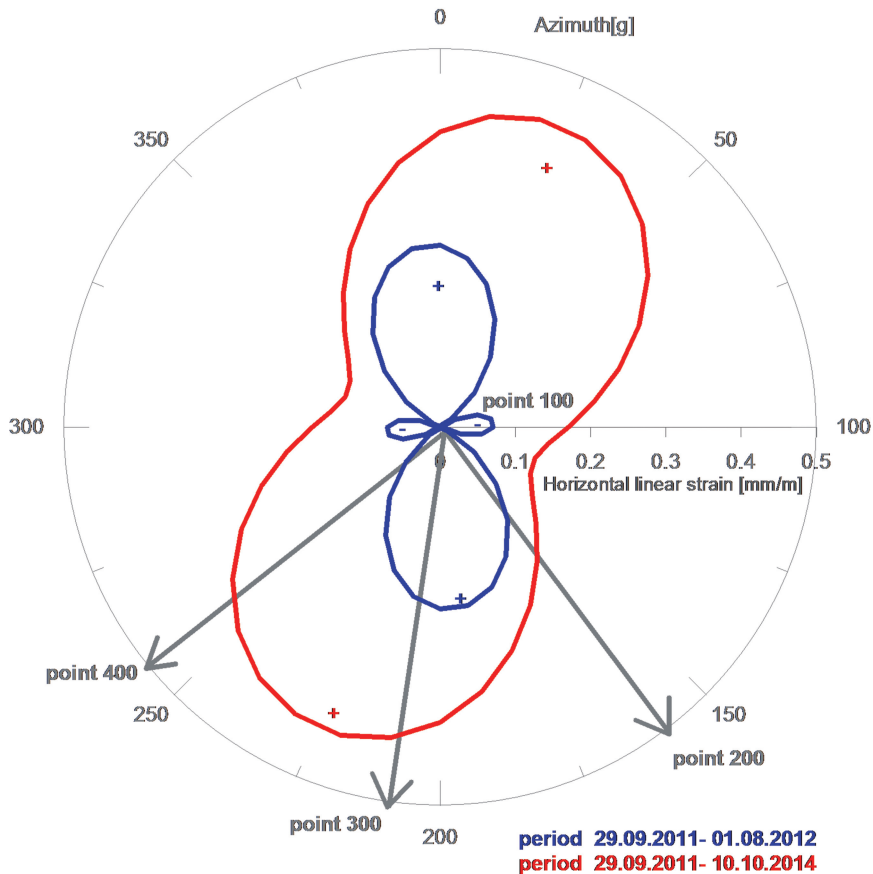


**Fig. 2.** Strain distribution in the rectangular rosette in Milówka

**Rys. 2.** Rozkład odkształceń w rozecie prostokątnej w Milówce

## 5. LANDSLIDE ON THE PERMANENT SLOPE OF THE OPENCAST MINE

The landslide labeled 24S, located on the permanent slope of the selected opencast mine, resulted from opencast mining operations became active in 2004, four months after a scarp in the pit was created. Morphomet-

ric parameters of the landslide have been presented in Table 5.

In the landslide area and in its immediate vicinity there are 20 points established, whose X, Y, H location is being determined by employees of the Surveying Department of the Mine in the cycles of 7–10 days using RTK GPS technology (Fig. 3).

**Table 5.** Morphometric parameters of the 24S landslide  
**Tabela 5.** Parametry morfometryczne osuwiska 24S

Parameter	
Area [ha]	24
Length [m]	580
Width [m]	594
Maximum height [m above sea level]	199
Minimum height [m above sea level]	120
Inclination [°]	16
Azimuth [°]	350

From among the existing points, four of them were selected, marked with the following numbers: 284, 344, 504, 505, to create the rosette with the central point 505. Three measurement series were selected, which were carried out on 2011-01-27 (series 1), 2012-01-30 (series 2), 2013-01-31 (series 3).

On the basis of the determined plane coordinates X, Y in the selected series, together with erroneousousness of the coordinates adopted at the level of  $\pm 1$  cm, the length of the sides of the rosette was calculated together with errors (Tab. 6).

The values of the calculated linear strains and strain tensor components have been summarized in Tab. 7 and Tab. 8.

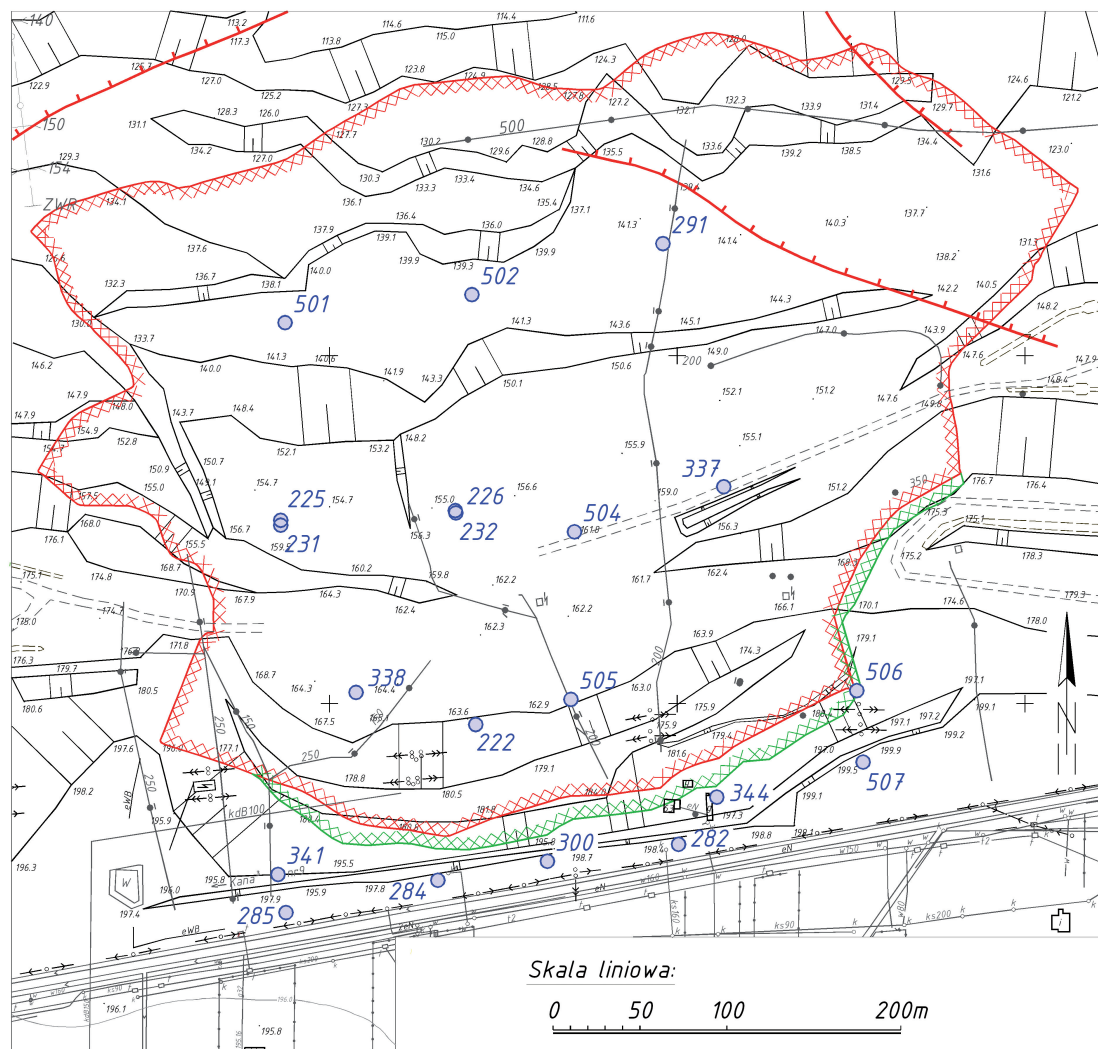


**Fig. 3.** Location of the points established in the 24S landslide area (Szafarczyk et al.)

**Rys. 3.** Usytuowanie punktów zastabilizowanych na terenie osuwiska 24S (Szafarczyk et al.)

**Table 6.** Summary of the calculated lengths of the sides of the central rosette located on the 24S landslide area, together with errors in each measurement series

**Tabela 6.** Zestawienie obliczonych długości boków rozety centralnej zlokalizowanej na terenie osuwiska 24S wraz z błędami w poszczególnych seriach pomiarowych

Side	Measurement series (date of performance)		
	I (27 I 2011)	II (30 I 2012)	III (31 I 2013)
505-504	97,059m±14mm	97,510m±14mm	97,744m±14mm
505-344	102,290m±14mm	103,076m±14mm	103,553m±14mm
505-284	131,156m±14mm	132,595m±14mm	133,432m±14mm

**Tab.7. Values** of linear strains on the sides of the central rosette (24S landslide location), with errors

**Tab. 7.** Wartości odkształceń liniowych na bokach rozety centralnej (osuwisko 24S) wraz z błędami

Side	Linear strain in the period I-II [mm/m] ± error [mm/m]	Linear strain in the period I-III [mm/m] ± error [mm/m]
505-504	4,64 ±0,83	7,05 ±1,16
505-344	7,68 ±1,20	12,34 ±1,81
505-284	10,97 ±1,28	17,35 ±1,93

**Tab. 8.** Strain tensor components determined for the state on January 30, 2012 and January 31, 2013 relative to the first measurement series performed on January 27, 2011 for the rosette (24S landslide location)

**Tab. 8.** Składowe tensora odkształcenia wyznaczone dla stanu w dniu 30 I 2012 oraz 31 I 2013 względem pierwszej serii pomiarowej wykonanej dnia 27 I 2011 (rozeta na osuwisku 24 S)

State as of (date)	$\epsilon_{11}$ [mm/m]	$\epsilon_{12} = \epsilon_{21}$ [mm/m]	$\epsilon_{22}$ [mm/m]	$\epsilon_{\max}$ [mm/m]	$\epsilon_{\min}$ [mm/m]	Gamma [-]	Beta [g]
2012-01-30	4,52	3,43	14,12	15,22	3,42	11,80	80,21
2013-01-31	6,86	5,47	22,82	24,51	5,16	19,35	80,87

The central rosette, located in the upper part of the landslide 24S, covering with its range the main scarp, revealed in both measurement periods only tensile strains.

The highest strain value was 24.51 mm/m in the measurement period I–III. The direction of the occurrence of extreme deformation, compatible for both of the determined states, was 80 gon and it is approximately perpendicular to the direction of the slope.

## 6. COMMENTS ON THE USE OF STRAIN GAUGE ROSETTES

The research studies carried out earlier (Kontny et al., 2014, Szafarczyk et al., 2013, Cai, 2001.) confirm that structures called rosettes, are successfully used to

determine the state of strain in extensive areas (sides of the rosettes with the lengths of several kilometers) as well as locally (sides of about 20 meters in length). Selection of the location of the established sides, or use of the already existing points, is of fundamental importance for the correct interpretation of the phenomenon and for the obtained results, consistent with the actual state of strain. According to the research studies carried out earlier by the author (Szafarczyk, 2013), the assumption made in geodetic measurements of strains, and relating to the homogeneity and continuity of the soil medium, is not fulfilled. This frequently results in obtaining various relative values of the linear strain on the same direction using measurement segments of various lengths.



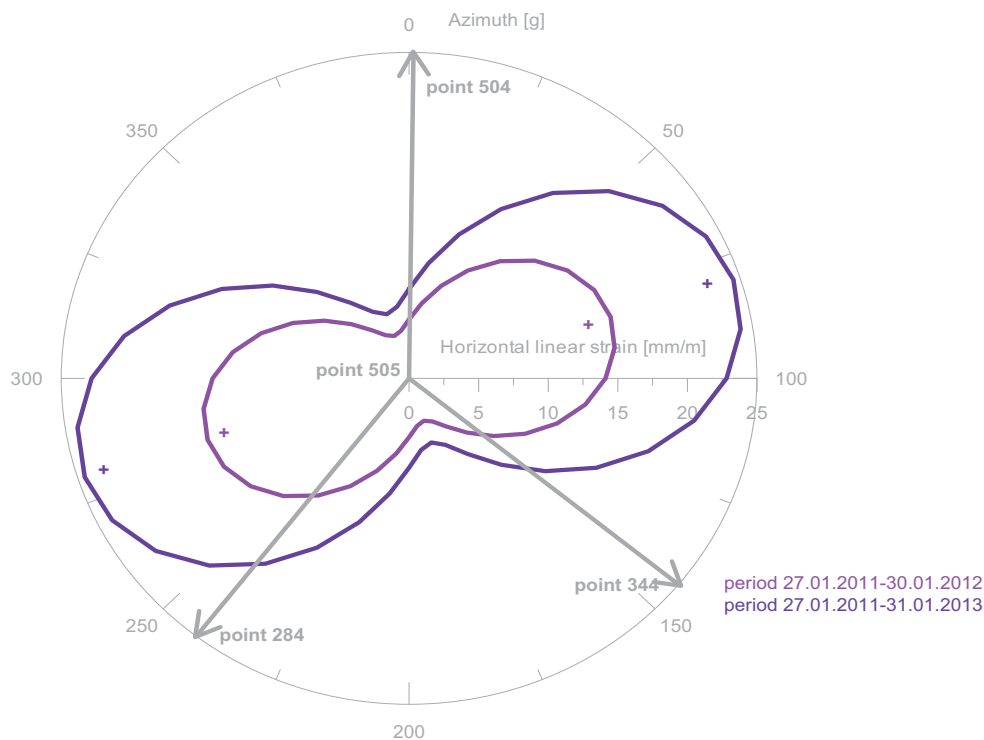


**Fig. 4.** Strain distribution in the central rosette located in 24S landslide area

**Rys. 4.** Rozkład odkształceń w rozecie centralnej zlokalizowanej na terenie osuwiska 24S

The two presented examples highlight the fact that the direction of the occurring extreme strains (in this case tensile strains), is not always consistent with the direction of the greatest slope. The fact that the direction of extreme strains is the same for the entire duration of the landslide process (or for the duration of the measurements performed on the landslide) is not a result of the high accuracy of the measurements or of the regularity of the process, but it is associated with the location of the rosette with respect to the source of the occurring strains. The presented methodology for determining the values of extreme strains is particularly useful in those areas where directions of extreme strains are variable in time. Therefore, it is preferred to position rosettes in the immediate vicinity of affected buildings, as it allows to determine whether the resulting damage was due to a landslide activity or is due to possible structural defects of the object.

The study should not be limited only to specifying the strain value, but it should always be complemented with the information on the accuracy of the performed calculations. Depending on the applied method for

measuring length, the same values of the strains may, or may not be, significant from a statistical point of view.

In the case of occurrence of significant strains, causing damage to buildings, land cracks, the occurrence of discontinuous strains can be used to analyze the value of the length determined from the coordinates.

In the case of slow deformation, of small values, a direct measurement of the lengths of segments should be performed, for which strains are determined.

## ACKNOWLEDGEMENTS

The article was created as part of the AGH statutory research of the Chair of Mine Areas Protection, Geoinformatics and Mine Surveying, number 11.11.150.195.

## REFERENCES

- Cai J.: 2001, Hypothesis test and sampling statistics of the eigenvalues and eigendirections of a random tensor of type deformation tensor, Report of DFG – Project GR 323/36-1 – Geodätisches Institut Universität Stuttgart, Lehrstuhl Statistik Universität, Dortmund.

- Ćmielewski B., Kontny B., Ćmielewski K.: 2013, Use of low-cost MEMS technology in early warning system against landslide threats. *Acta Geodyn. Geomater.*, Vol. 10, No. 4 (172), 485–490. DOI: 10.13168/AGG.2013.0049.
- Dong J., Lee W., Lin M., Huang A., Lee Y.: 2009, Effects of seismic anisotropy and geological characteristics on the kinematics of the neighboring Jiufengershan and Hungtsaping landslides during Chi-Chi earthquake, *Tectonophysics*, Vol. 466, Issues 3–4, pp. 438–457, DOI:10.1016/j.tecto.2007.11.008.
- Gili J.A., Corominas J., Rius J.: 2000, Using Global Positioning System techniques in landslide monitoring, *Engineering Geology*, Vol. 55, Issue 3, pp. 167–192. DOI:10.1016/S0013-7952(99)00127-1.
- Gustkiewicz J.: 1980, Metody tensometryczne i fleksimetryczne (in Polish) In: „Ochrona powierzchni przed szkodami górniczymi”. M. Borecki, ed. Wydawnictwo Śląsk. Katowice. 967 p.
- Hejmanowski R.: 2005, Optimization of determining horizontal surface deformations for the protection of buildings in mining areas. (In Polish). Report of Research Project 5T 12E 04124, Akademia Górniczo-Hutnicza, Kraków.
- Kajetanowicz P., Wierzejewski J.: 2008, Algebra z geometrią analityczną (In Polish), Wydawnictwo Naukowe PWN, p. 178.
- Kontny B., Grzempowski P., Aleksandrowski P., Schenk V., Schenková Z.: 2014, Horizontal deformation of the earth's crust in the area of Sudeten and its northern foreland (SW Poland) based on GPS data from the period 1997–2012, In: 15<sup>th</sup> Czech-Polish Workshop “On Recent Geodynamics of the Sudeten and Adjacent Areas”, Karlov po Praděem, Czech Republic, November 5–8, Conference proceedings, pp. 40–41.
- Kostić S., Vasović N., Franović I., Jevremović D., Mitrinović D., Todorović K.: 2014, Dynamics of landslide model with time delay and periodic parameter perturbations, *Communications in Nonlinear Science and Numerical Simulation*, Vol. 19, Issue 9, pp. 3346–3361. DOI:10.1016/j.cnsns.2014.02.012.
- Kwinta A.: 2012, Prediction of strain in a shaft caused by underground mining, *International Journal of Rock Mechanics and Mining Sciences*, Vol. 55, pp. 28–32. DOI:10.1016/j.ijrmms.2012.06.007.
- McColl S.T.: 2015, Landslide Causes and Triggers, *Landslide Hazards, Risks and Disasters Chapter 2*, pp. 17–42. DOI:10.1016/B978-0-12-396452-6.00002-1.
- Okamoto T., Larsen J. O., Matsuura S., Asano S., Takeuchi Y., Grande L.: 2004, Displacement properties of landslide masses at the initiation of failure in quick clay deposits and the effects of meteorological and hydrological factors, *Engineering Geology*, Vol. 72, Issues 3–4, pp. 233–251. DOI:10.1016/j.enggeo.2003.09.004.
- Pałka P., Skulich M.: 2013, Analiza obserwacji kątowno-liniowych w aspekcie wyznaczania odkształceń terenu osuwiskowego. *Infrastruktura i Ekologia Terenów Wiejskich*. Nr 2013/ 03 (2 (Sep 2013))
- Pielok J., Szafarczyk A.: 2004, Geodetic measurements of surface deformations with the use of tensometry methods, *Das Markscheidewesen*, Vol. 111, nr 3, pp. 98–103, ISSN 0174-1357.
- Prokešová R., Kardoš M., Medved'ová A.: 2010, Landslide dynamics from high-resolution aerial photographs: A case study from the Western Carpathians, Slovakia, *Geomorphology*, Vol. 115, Issues 1–2, pp. 90–101. DOI:10.1016/j.geomorph.2009.09.033.
- Ramesh M., V.: 2014, Design, development, and deployment of a wireless sensor network for detection of landslides, *Ad Hoc Networks*, Vol. 13, Part A, pp. 2–18, DOI:10.1016/j.adhoc.2012.09.002.
- Szafarczyk, A.: 2013, Determination of horizontal deformations of the mining area using geodetic rosettes (in Polish), *Wydawnictwa AGH*, e-ISBN: 978-83-7464-573-7, 144 p.
- Szafarczyk, A. Rybicki S. et al: 2013, Study of the kinematics of surface mass movements using ground-based radar interferometry (in Polish), *Wydawnictwa AGH*, ISBN: 978-83-7464-648-2, 126 p.
- Teza G., Pesci A., Rinaldo G., Galgaro A.: 2008, Characterization of landslide ground surface kinematics from terrestrial laser scanning and strain field computation, *Geomorphology*, Vol. 97, Issues 3–4, pp. 424–437, DOI:10.1016/j.geomorph.2007.09.003.
- Wang K.L., Lin M.L.: 2011, Initiation and displacement of landslide induced by earthquake — a study of shaking table model slope test, *Engineering Geology*, Vol. 122, Issues 1–2, pp. 106–114. DOI:10.1016/j.enggeo.2011.04.008.
- Wanic A.: 2007, *Instrumentoznawstwo geodezyjne i elementy technik pomiarowych (in Polish)* Wydawnictwo Uniwersytetu Warmińsko-Mazurskiego w Olsztynie, 458 p.
- Wasowski J., Bovenga B.: 2015, Remote Sensing of Landslide Motion with Emphasis on Satellite Multitemporal Interferometry Applications: An Overview, *Landslide Hazards, Risks and Disasters Chapter 11*, Pages 345–403. DOI:10.1016/B978-0-12-396452-6.00011-2.
- Yenes M., Monterrubio S., Nespereira J., Santosc G.: 2009, Geometry and kinematics of a landslide surface in tertiary clays from the Duero Basin (Spain), *Engineering Geology*, Vol. 104, Issues 1–2, pp. 41–54. DOI:10.1016/j.enggeo.2008.08.008.
- Stumpf A., Malet J.F., Kerle N., Niethammer U., Rothmund S.: 2013, Image-based mapping of surface fissures for the investigation of landslide dynamics, *Geomorphology*, Vol., pp. 12–27. DOI:10.1016/j.geomorph.2012.12.010.
- Zhu Z.W., Liu D.Y., Yuan Q.Y., Liu B., Liu J.C.: 2011, A novel distributed optic fiber transducer for landslides monitoring, *Optics and Lasers in Engineering*, Vol. 49, Issue 7, pp. 1019–1024. DOI:10.1016/j.optlaseng.2011.01.010.